Accepted Manuscript

International Journal of Modern Physics E

Article Title:	Testing the Core-Cluster Model Calculations for Some Heavy Deformed Nuclei
Author(s):	L. I. Abou-Salem, K. E. Abdelmageed, I. A. Elmashad, R. Al Allam
DOI:	10.1142/S0218301319500496
Accepted:	17 July 2019
To be cited as:	L. I. Abou-Salem *et al.*, Testing the Core-Cluster Model Calculations for Some Heavy Deformed Nuclei, *International Journal of Modern Physics E*, doi: 10.1142/S0218301319500496
Link to final version:	https://doi.org/10.1142/S0218301319500496

World Scientific
www.worldscientific.com

Testing the Core-Cluster Model Calculations for Some Heavy Deformed Nuclei

L. I. Abou-Salem,* K. E. Abdelmageed,† I. A. Elmashad,‡ and R. Al Allam§
Physics Department, Faculty of Science, Benha University, Benha 13518, Egypt

In the present work, the spectra of some even-even isotopes are studied through selecting of core-cluster decomposition of the parent nucleus. The considered nuclei lie in the rare-earth and the transition metal regions. The Schrödinger equation can be solved using Bohr-Sommerfeld relation and the modified Woods-Saxon beside Coulomb potentials to reproduce the spectra of these isotopes with mass number ($154 \leq A \leq 168$). The theoretical calculations of the excitation energies of the ground-state rotational band are compared to the experimental data. The cluster model calculations show a good agreement with the experimental data for the transitional and rotational nuclei more than the vibrational nuclei. Some negative parity bands of the chosen nuclei are studied. The core-cluster charge products are correlated with the transition probability $B(E2 : 2^+ \rightarrow 0^+)$.

Keywords: Core-Cluster Model ; Correlation ; Heavy Nuclei ;Bohr-Sommerfeld Quantization

I. INTRODUCTION

The cluster model of nuclear structure is well established for light nuclei [1–3]. The presence of alpha -particle cluster states in light nuclei has been agreeable for a long time [1]. Many indications showed that the nuclear cluster can be applied to the actinide and the rare-earth deformed nuclei [4–11]. The cornerstone of this model is that the parent nucleus can be treated as two component nuclei, i.e. two-body system, each of them has its own state characteristics and interacting through a local deep potential [12].The choice of core-cluster decomposition can be executed by many methods. One of them was proposed by Buck [13], in which the main criterion of the core-cluster selection is dependance on available information of experimental and theoretical binding energies for both core and cluster. The energy levels of the ground-state rotational bands of many actinide nuclei are well reproduced using a binary cluster model [14].The spectra of even-even nuclei and the transition probability have been studied for the transition element isotopes of Hf [15]. The properties of alternating parity bands in actinides and Ce, Ba, and Nd isotopes have been explained [8]. Also, it was able to calculate the rotational bands and the electric dipole transitions between the parity doublet members [9]. For the first time, the low-lying alternative parity band were predicted in the heaviest nuclei and many properties were studied for these heavy nuclei [10]. The multiple negative and positive parity rotational bands in ^{240}Pu were described [11]. We attempt to study the ground-state rotational band of some transition metal region nuclei with mass number ($88 \leq A_T \leq 118$) using the core-cluster model[16].

In the present work, the ground-state rotational band of some even-even nuclei ($^{154-160}Dy$, $^{156-162}Er$, $^{158-164}Yb$, $^{160-166}Hf$, and $^{162-168}W$) in the rare-earth and transition metal regions are studied using the cluster model.
The outline of the paper is as follows, in section II, we discuss the cluster model beginning with the selection of the even-even core and cluster for the chosen nuclei and study the spectra of the selected nuclei. Section III is devoted to the results and discussion.

*Electronic address: loutfy.Abousalem@fsc.bu.edu.eg
†Electronic address: karima.abdelmagid@fsc.bu.edu.eg
‡Electronic address: ibrahim.elmashad@fsc.bu.edu.eg
§Electronic address: alyasabdul2012@gmail.com

II. THE USED MODEL

A. Choice of the Core-Cluster

The general method of selecting core and cluster is to choose the possible preference combinations that have internal stability [17], so that an even-even nucleus of mass and charge (A_T, Z_T) should be split into an even-even core (A_1, Z_1) and cluster (A_2, Z_2) such that the function $D(1,2)$ is maximized as:

$$D(1,2) = [B_A(Z_1, A_1) - B_L(Z_1, A_1)] + [B_A(Z_2, A_2) - B_L(Z_2, A_2)] \tag{1}$$

Where $(1,2)$ refer to the core and cluster, respectively. B_A is the actual binding energy and B_L is a liquid drop binding energy which given by:

$$B_L = a_v A - a_s A^{2/3} - a_c Z^2 A^{-1/3} - \frac{a_a (A-2Z)^2}{A} + \delta \tag{2}$$

With $a_v = 15.56$, $a_s = 17.23$, $a_c = 0.697$, $a_a = 23.285$, and $\delta = 12A^{-1/2}$ with all values in MeV. For the selected nucleus, when the conditions $A_1 = A_T - A_2$ and $Z_1 = Z_T - Z_2$ are applied, D remains a function of two independent variables; the cluster mass and charge, (A_2, Z_2). Moreover, electric dipole transitions between low-lying bands of opposite parity in heavy nuclei are very weak. This implies that, the total nuclear mass and charge should be distributed in the same proportion between the core and cluster, resulting in the no-dipole constraint [18],

$$\frac{Z_1}{A_1} = \frac{Z_2}{A_2} = \frac{Z_T}{A_T} \tag{3}$$

B. Spectra of Even-Even Nuclei

The Schrödinger equation can be solved using Bohr-Sommerfeld relation. Hence, we can generate the spectra $E(G, L)$ of the core-cluster decompositions [19]:

$$\int_{r_1}^{r_2} \sqrt{\frac{2\mu}{\hbar^2}\left[E(G,L) - \left[V_N(r,R) + V_C(r,R) + \frac{\hbar^2(L+1/2)^2}{2\mu r^2}\right]\right]} = (G - L + 1)\frac{\pi}{2} \tag{4}$$

where r_1 and r_2 are the two inner most classical turning points, μ is the relative mass of the core-cluster decomposition, G is the global quantum number identifying the band levels given by $G = 2n + L$, L is the angular momentum of particular level and n is the number of nodes in the radial wave function of the core-cluster relative motion [20]. For the selected nuclei, in case of positive parity nuclei, we set $G = 4A_2$ with A_2 the cluster mass, this is appropriate in the present calculations [18]. We study some negative parity bands using the global quantum number G is one unit larger than for the positive parity bands [21].
The core-cluster interaction in Eq. (4) includes nuclear and Coulomb terms. For the nuclear interaction $V_N(r, R)$ the modified Woods-Saxon potential [22] is used,

$$V_N(r,R) = -\left(\frac{A_1 A_2}{A}\right)\frac{f(r,R,x,a)}{f(0,R,x,a)}V_0 \tag{5}$$

with,

$$f(r,R,x,a) = \left[\frac{x}{1 + exp((r-R)/a)} + \frac{1-x}{(1+exp((r-R)/3a))^2}\right]$$

where V_0 is the nuclear potential depth, a is nonzero diffuseness and R is the radius of core.
The Coulomb potential V_C is taken as [5],

$$V_C(r,R) = \frac{Z_1 Z_2 e^2}{r} \qquad for \quad r \geq R \tag{6}$$

$$= \frac{Z_1 Z_2 e^2}{2R}\left[3 - \left(\frac{r}{R}\right)^2\right] \qquad for \quad r \leq R \tag{7}$$

C. Correlations

In this section, we discuss the Correlations between the core-cluster products (Z_1Z_2/Z_T) and the transition probability $B(E2:2^+\rightarrow 0^+)$. The expression for $B(E2:2^+\rightarrow 0^+)$ is given by [23]:

$$B(E2)=\frac{1}{4\pi}\left[\frac{Z_1Z_2}{Z_T}\int x_\lambda(r)r^2x_0(r)dr\right]^2 \tag{8}$$

Where $x_\lambda(r)$ is the radial wave function of the core-cluster relative motion for angular momentum λ. For near-identical x_λ [6], we can then write:

$$\frac{\sqrt{B(E2)}}{A_T^{2/3}}=\frac{1}{\sqrt{4\pi}}r_0^2\left(\frac{Z_1Z_2}{Z_T}\right) \tag{9}$$

We replace Eq. (9) by less restricted forms

$$\frac{\sqrt{B(E2)}}{A_T^{2/3}}=a_0+\frac{1}{\sqrt{4\pi}}r_0^2\left(\frac{Z_1Z_2}{Z_T}\right) \tag{10}$$

where a_0 is a parameter that can be determined from plotting the relation between the transition probability $\sqrt{B(E2)}/A_T^{2/3}$ and Z_1Z_2/Z_T.

III. RESULTS AND DISCUSSION

One can divide the considered even-even nuclei into three regions according to the value of R_4. Where R_4 is the ratio between E_4^+ and E_2^+ of the ground-state rotational band. From this ratio we can determine some properties of the considered nucleus. The ratio R_4 takes values ($3.0 < R_4 < 3.33$) for the rotational region, while for vibrational region is ($2.0 < R_4 < 2.4$). The R_4 of the transitional region have intermediate value between vibrational and rotational region ($2.4 < R_4 < 3.0$) [24]. In the present work, the nuclei ($^{154-160}Dy$, $^{156-162}Er$, $^{158-164}Yb$, $^{160-166}Hf$, and $^{162-168}W$) are considered. These nuclei represent both rare-earth and transition metal nuclei as shown in Table(I). One can notice that, the rare-earth nuclei ($_{66}Dy$, $_{68}Er$, and $_{70}Yb$) transfer from vibrational to rotational region. It is obvious from Table(I), the isotopes of these elements are varied from vibrational to rotational region by increasing the number of neutrons (from 88 to 94). While in transition metal nuclei ($_{72}Hf$ and $_{74}W$), the considered isotopes are varied from vibrational to transitional region by increasing the neutrons number (from 88 to 94).

Tab. I: R_4 values for the chosen Even-Even Nuclei.

Isotopes ⇓	**Isotones ⇒**				
	$^{154}_{66}Dy$	$^{156}_{68}Er$	$^{158}_{70}Yb$	$^{160}_{72}Hf$	$^{162}_{74}W$
$R_4=E_4/E_2$	2.23	2.314	2.331	2.306	2.252
	$^{156}_{66}Dy$	$^{158}_{68}Er$	$^{160}_{70}Yb$	$^{162}_{72}Hf$	$^{164}_{74}W$
$R_4=E_4/E_2$	2.9	2.743	2.626	2.559	2.478
	$^{158}_{66}Dy$	$^{160}_{68}Er$	$^{162}_{70}Yb$	$^{164}_{72}Hf$	$^{166}_{74}W$
$R_4=E_4/E_2$	3.2	3.099	2.923	2.786	2.681
	$^{160}_{66}Dy$	$^{162}_{68}Er$	$^{164}_{70}Yb$	$^{166}_{72}Hf$	$^{168}_{74}W$
$R_4=E_4/E_2$	3.27	3.23	3.127	2.966	2.821

Also, this table shows that isotones with ($N = 94$ and $66 \leq Z \leq 70$), the rare earth nuclei are rotational nuclei. However, the transition metal nuclei with ($N = 94$ and $72 \leq Z \leq 74$) are transitional nuclei. We have studied the experimental data [25] to determine the levels of the ground-state rotational band of the considered nuclei using the relation between the moment of inertia $\left(2\jmath/\hbar^2\right)$ and the square of the angular frequency $(\hbar\omega)^2$ [see fig. (1)]. There is a strong evidence for anomalous behavior of the moment of inertia at ($I^\pi \geq 6^+$) for the considered nuclei. Also, one can notice that, these anomalies are reduced with increasing the mass number.

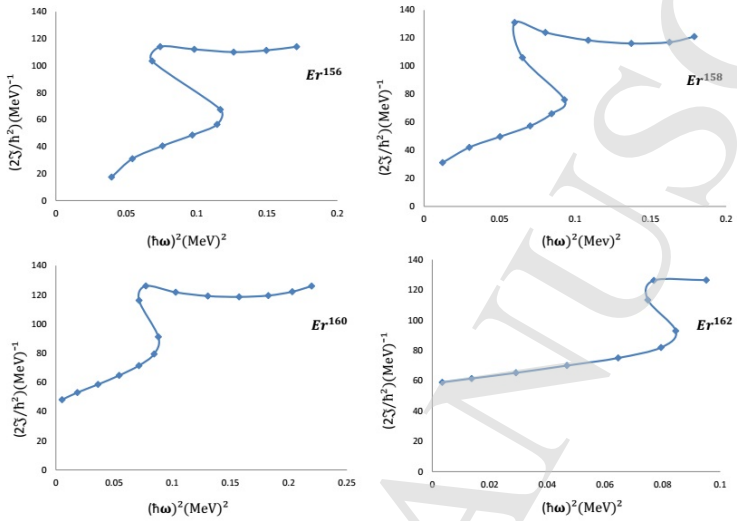

Fig. 1: The relation between the moment of inertia $\left(\frac{2\jmath}{\hbar^2}\right)$, and the square of angular frequency $(\hbar\omega)^2$.

We selected the appropriate core-cluster decomposition for considered isotopes in rare-earth and transition metal nuclei using Eqs.(1) and (2). The experimental binding energies for different nuclei are taken from Ref. [26]. We calculated $D(1,2)$ as a function of the cluster charge Z_2 using Eq.(1). Fig.(2) represents the plotting of the function $D(1,2)$ versus the cluster charge Z_2.

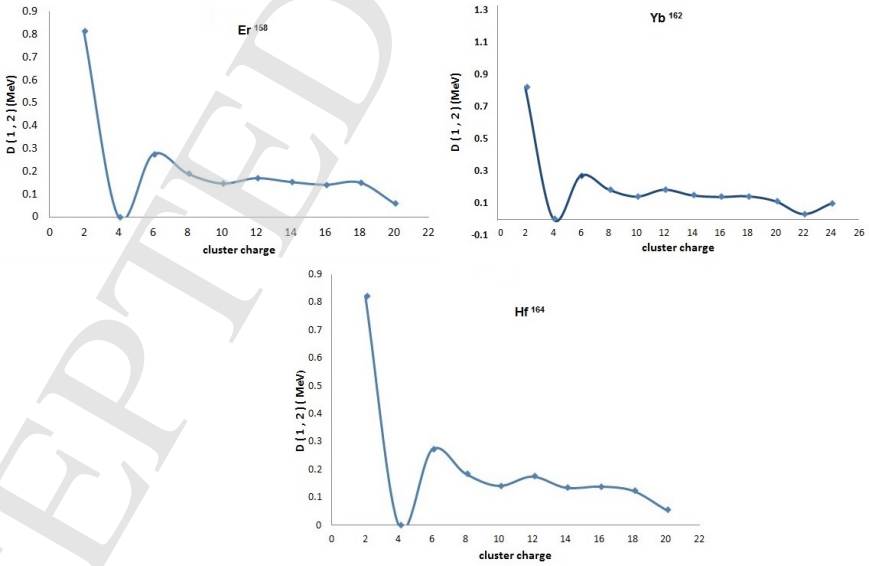

Fig. 2: $D(1,2)$ as a function of cluster charge Z_2 for some considered nuclei.

From this fig. (2), one can notice that, there are two maxima at $Z_2 = 2$ and 6. Therefore, clusters ^{12}C and ^{14}C are considered according to the decompositions given in table(II).

Tab. II: The decompositions of the chosen parent nuclei.

Nucleus	First decomposition	Second decompositions
$^{154}_{66}Dy$	$^{142}_{60}Nd + ^{12}_{6}C$	$^{140}_{60}Nd + ^{14}_{6}C$
$^{156}_{66}Dy$	$^{144}_{60}Nd + ^{12}_{6}C$	$^{142}_{60}Nd + ^{14}_{6}C$
$^{158}_{66}Dy$	$^{146}_{60}Nd + ^{12}_{6}C$	$^{144}_{60}Nd + ^{14}_{6}C$
$^{160}_{66}Dy$	$^{148}_{60}Nd + ^{12}_{6}C$	$^{146}_{60}Nd + ^{14}_{6}C$
$^{156}_{68}Er$	$^{144}_{62}Sm + ^{12}_{6}C$	$^{142}_{62}Sm + ^{14}_{6}C$
$^{158}_{68}Er$	$^{146}_{62}Sm + ^{12}_{6}C$	$^{144}_{62}Sm + ^{14}_{6}C$
$^{160}_{68}Er$	$^{148}_{62}Sm + ^{12}_{6}C$	$^{146}_{62}Sm + ^{14}_{6}C$
$^{162}_{68}Er$	$^{150}_{62}Sm + ^{12}_{6}C$	$^{148}_{62}Sm + ^{14}_{6}C$
$^{158}_{68}Yb$	$^{146}_{64}Gd + ^{12}_{6}C$	$^{144}_{64}Gd + ^{14}_{6}C$
$^{160}_{68}Yb$	$^{148}_{64}Gd + ^{12}_{6}C$	$^{146}_{64}Gd + ^{14}_{6}C$
$^{162}_{68}Yb$	$^{150}_{64}Gd + ^{12}_{6}C$	$^{148}_{64}Gd + ^{14}_{6}C$
$^{164}_{68}Yb$	$^{152}_{64}Gd + ^{12}_{6}C$	$^{150}_{64}Gd + ^{14}_{6}C$
$^{160}_{72}Hf$	$^{148}_{66}DY + ^{12}_{6}C$	$^{146}_{66}DY + ^{14}_{6}C$
$^{162}_{72}Hf$	$^{150}_{66}DY + ^{12}_{6}C$	$^{148}_{66}DY + ^{14}_{6}C$
$^{164}_{72}Hf$	$^{152}_{66}DY + ^{12}_{6}C$	$^{150}_{66}DY + ^{14}_{6}C$
$^{166}_{72}Hf$	$^{154}_{66}DY + ^{12}_{6}C$	$^{152}_{66}DY + ^{14}_{6}C$
$^{162}_{74}W$	$^{150}_{68}Er + ^{12}_{6}C$	$^{148}_{68}Er + ^{14}_{6}C$
$^{164}_{74}W$	$^{152}_{68}Er + ^{12}_{6}C$	$^{150}_{68}Er + ^{14}_{6}C$
$^{166}_{74}W$	$^{154}_{68}Er + ^{12}_{6}C$	$^{152}_{68}Er + ^{14}_{6}C$
$^{168}_{74}W$	$^{156}_{68}Er + ^{12}_{6}C$	$^{154}_{68}Er + ^{14}_{6}C$

The energy levels of the ground-state rotational band for the considered nuclei can be obtained from solving Eq. (4) numerically. The modified Wood-Saxon potential parameters are taken as; $V_0 = 55 \pm 1$ MeV, $a = 0.735 \pm 0.005$fm, $x = 0.335 \pm 0.005$, while the core of radius R is considered as free parameter which is adjusted through the $\chi^2 - test$. Tables(III) to (VII) show the comparison between the calculated energy levels of the ground-state rotational band and their corresponding experimental data [25] for the considered nuclei.

Table(III) represents the comparison between the experimental data and the theoretical values of $^{154-160}Dy$ isotopes. The ground-state rotational band is up to $I^\pi \sim 16^+$ in $^{154-160}Dy$ isotopes. This table shows that a satisfied agreement between the experimental and theoretical values exist. The deviation between the experimental and theoretical values increase at $I^\pi \geq 14^+$, however, a good agreement can be shown in case of $^{156-158}Dy$ isotopes at $I^\pi \leq 16^+$, which lie in the transitional and rotational regions according to its R_4 values.

Tab. III: Shows the comparison between the calculated energy levels of the ground-state rotational band in MeV and their corresponding experimental data for $^{154-160}Dy$ [25].

Excitation Energy	^{154}Dy			^{156}Dy			^{158}Dy			^{160}Dy		
I^{π}	Exp.	^{12}C	^{14}C	*Exp.*	^{12}C	^{14}C	*Exp.*	^{12}C	^{14}C	*Exp.*	^{12}C	^{14}C
0^+	0	0	0	0	0	0	0	0	0	0	0	0
2^+	0.334	0.556	0.266	0.138	0.171	0.246	0.099	0.111	0.230	0.087	0.080	0.241
4^+	0.747	0.792	0.636	0.404	0.416	0.541	0.317	0.370	0.533	0.284	0.340	0.546
6^+	1.224	1.161	0.964	0.770	0.788	0.782	0.638	0.698	0.749	0.581	0.672	0.757
8^+	1.747	1.627	1.487	1.216	1.246	1.137	1.044	1.141	1.109	0.967	1.120	1.112
10^+	2.304	2.186	2.082	1.725	1.815	1.537	1.520	1.634	1.535	1.428	1.599	1.547
12^+	2.893	2.746	2.820	2.286	2.369	2.079	2.049	2.197	2.039	1.950	2.175	2.031
14^+	3.509	3.408	3.543	2.887	3.035	2.547	2.612	2.784	2.568	2.513	2.768	2.574
16^+	4.090	4.126	4.390	3.523	3.738	3.125	3.190	3.441	3.137	3.089	3.437	3.172
$\chi^2 - test$		0.121	0.197		0.035	0.227		0.070	0.185		0.143	0.301

Table (IV) shows the calculated values compared with the experimental ones of $^{156-162}Er$ isotopes. The ground-state rotational band up to $I^{\pi} \sim 16^+$ in $^{156-162}Er$ isotopes. One can notice that, there is more agreement in the lowest excited state levels of Er-isotopes except for ^{156}Er. The deviation between the experimental and calculated values increases at $I^{\pi} \geq 12^+$. Also, this table shows a good agreement between the experimental and theoretical values in case of $^{158-162}Er$ isotopes, which lie in the transitional and rotational regions.

Tab. IV: Shows the comparison between the calculated energy levels of the ground-state rotational band in MeV and their corresponding experimental data for $^{156-162}Er$ [25].

Excitation Energy	^{156}Er			^{158}Er			^{160}Er			^{162}Er		
I^{π}	Exp.	^{12}C	^{14}C	*Exp.*	^{12}C	^{14}C	*Exp.*	^{12}C	^{14}C	*Exp.*	^{12}C	^{14}C
0^+	0	0	0	0	0	0	0	0	0	0	0	0
2^+	0.345	0.556	0.682	0.192	0.186	0.201	0.126	0.093	0.079	0.102	0.121	0.133
4^+	0.797	0.898	1.020	0.527	0.539	0.529	0.389	0.391	0.413	0.330	0.362	0.438
6^+	1.341	1.285	1.337	0.970	0.912	0.853	0.765	0.760	0.744	0.667	0.721	0.647
8^+	1.959	1.810	1.831	1.493	1.429	1.353	1.229	1.239	1.241	1.097	1.178	1.000
10^+	2.633	2.346	2.332	2.072	1.976	1.860	1.761	1.757	1.736	1.603	1.742	1.409
12^+	3.314	2.997	2.959	2.680	2.629	2.476	2.340	2.374	2.373	2.165	2.284	1.897
14^+	3.836	3.676	3.649	3.190	3.314	3.151	2.932	3.051	3.036	2.745	2.928	2.411
16^+	4.380	4.443	4.385	3.663	4.077	3.910	3.466	3.792	3.796	3.292	3.620	2.967
$\chi^2 - test$		0.183	0.316		0.059	0.088		0.044	0.061		0.073	0.190

Table (V) represents the comparison between the experimental data and the theoretical values of $^{158-164}Yb$ isotopes. The ground-state rotational band is up to $I^{\pi} \sim 16^+$ in $^{158-164}Yb$ isotopes. This table shows that a good agreement between the experimental and theoretical values except in case of ^{158}Yb, which lie in the vibrational region.

Tab. V: Shows the comparison between the calculated energy levels of the ground-state rotational band in MeV and their corresponding experimental data for $^{158-164}Yb$ [25].

Excitation Energy	^{158}Yb			^{160}Yb			^{162}Yb			^{164}Yb		
I^{π}	Exp.	^{12}C	^{14}C	*Exp.*	^{12}C	^{14}C	*Exp.*	^{12}C	^{14}C	*Exp.*	^{12}C	^{14}C
0^{+}	0	0	0	0	0	0	0	0	0	0	0	0
2^{+}	0.358	0.673	0.725	0.243	0.393	0.427	0.167	0.216	0.226	0.123	0.157	0.075
4^{+}	0.835	1.005	1.063	0.638	0.727	0.763	0.487	0.552	0.562	0.386	0.418	0.412
6^{+}	1.403	1.384	1.384	1.147	1.100	1.088	0.924	0.921	0.882	0.760	0.761	0.738
8^{+}	2.047	1.895	1.883	1.736	1.620	1.593	1.446	1.448	1.381	1.223	1.215	1.250
10^{+}	2.743	2.415	2.382	2.373	2.141	2.097	2.024	1.974	1.880	1.753	1.766	1.739
12^{+}	3.426	3.051	3.013	2.959	2.777	2.721	2.634	2.613	2.493	2.330	2.284	2.381
14^{+}	3.934	3.745	3.695	3.363	3.460	3.392	3.257	3.276	3.145	2.899	2.920	3.039
16^{+}	4.502	4.475	4.446	3.847	4.192	4.164	3.879	4.016	3.915	3.388	3.569	3.808
$\chi^2 - test$		0.289	0.377		0.147	0.197		0.025	0.054		0.020	0.086

From the previous tables, one can notice that the agreement between the experimental and theoretical values increases with increasing the mass number of these isotopes. Also, the agreement between the experimental and the theoretical values manifest a weak agreement in the vibrational nuclei as ^{154}Dy, ^{156}Er, and ^{158}Yb, while the agreement gets better in the transitional and rotational nuclei such as ^{156}DY, ^{160}Er, and ^{164}Yb.

Table (VI) shows the comparison between the calculated and experimental values of $^{160-166}Hf$ isotopes. The ground-state rotational band is up to $I^{\pi} \sim 16^{+}$ in $^{160-166}Hf$ isotope. From this table, one can notice a satisfied agreement between the theoretical and experimental values except for ^{160}Hf. The deviations between the calculated results and experimental data decrease when the considered isotopes varied from the vibrational to transitional region through increasing the neutrons number.

Tab. VI: Shows the comparison between the calculated energy levels of the ground-state rotational band in MeV and their corresponding experimental data for $^{160-166}Hf$ [25].

Excitation Energy	^{160}Hf			^{162}Hf			^{164}Hf			^{166}Hf		
I^{π}	Exp.	^{12}C	^{14}C	*Exp.*	^{12}C	^{14}C	*Exp.*	^{12}C	^{14}C	*Exp.*	^{12}C	^{14}C
0^{+}	0	0	0	0	0	0	0	0	0	0	0	0
2^{+}	0.389	0.778	0.812	0.285	0.510	0.613	0.202	0.331	0.346	0.158	0.178	0.194
4^{+}	0.898	1.098	1.132	0.729	0.826	0.940	0.587	0.666	0.684	0.470	0.500	0.525
6^{+}	1.493	1.457	1.453	1.293	1.197	1.271	1.085	1.023	1.001	0.897	0.864	0.846
8^{+}	2.147	1.961	1.948	1.940	1.697	1.754	1.669	1.542	1.495	1.406	1.379	1.352
10^{+}	2.814	2.478	2.432	2.635	2.214	2.251	2.304	2.042	1.988	1.971	1.896	1.831
12^{+}	3.474	3.098	3.054	3.185	2.835	2.868	2.870	2.665	2.609	2.566	2.521	2.460
14^{+}	4.076	3.801	3.742	3.566	3.540	3.538	3.209	3.362	3.268	3.009	3.183	3.110
16^{+}	4.735	4.488	4.454	4.067	4.223	4.279	3.677	4.052	4.015	3.449	3.895	3.866
$\chi^2 - test$		0.373	0.450		0.280	0.355		0.154	0.200		0.070	0.081

Table (VII) represents the comparison between the experimental and the theoretical values of $^{162-168}W$ isotopes. The ground-state rotational band is up to $I^{\pi} \sim 16^{+}$ in $^{162-168}W$ isotope. From this table, one can notice a good agreement between the theoretical and experimental values in case of $^{166-168}W$ isotopes, which lie in the transitional region.

Tab. VII: Shows the comparison between the calculated energy levels of the ground-state rotational band in MeV and their corresponding experimental data for $^{162-168}W$ [25].

Excitation Energy	^{162}W			^{164}W			^{166}W			^{168}W		
I^{π}	Exp.	^{12}C	^{14}C	*Exp.*	^{12}C	^{14}C	*Exp.*	^{12}C	^{14}C	*Exp.*	^{12}C	^{14}C
0^+	0	0	0	0	0	0	0	0	0	0	0	0
2^+	0.449	0.870	0.942	0.332	0.656	0.650	0.252	0.438	0.281	0.199	0.292	0.409
4^+	1.012	1.165	1.263	0.822	1.021	0.975	0.676	0.749	0.606	0.562	0.609	0.709
6^+	1.638	1.522	1.568	1.429	1.367	1.335	1.226	1.109	0.964	1.042	0.964	1.081
8^+	2.267	2.013	2.038	2.115	1.857	1.817	1.865	1.602	1.450	1.600	1.466	1.573
10^+	2.823	2.528	2.518	2.830	2.428	2.421	2.551	2.108	2.055	2.202	1.967	2.177
12^+	3.442	3.138	3.112	3.438	3.096	3.083	3.031	2.717	2.724	2.817	2.575	2.834
14^+	4.122	3.807	3.811	3.830	3.769	3.847	3.356	3.403	3.495	3.419	3.275	3.591
16^+	4.851	4.529	4.463	4.338	4.523	4.668	3.821	4.082	4.297	4.003	3.936	4.433
$\chi^2 - test$		0.377	0.466		0.351	0.369		0.289	0.410		0.110	0.191

Table (VIII) shows the calculations of the energy levels of some negative parity bands of some selected nuclei and their corresponding experimental data [25]. The considered nuclei are ^{154}Dy, ^{156}Er, ^{164}Yb, ^{164}Hf, and ^{166}W. The predicted values of some negative energy states are given. One can notice a good agreement between the theoretical and experimental values in case of ^{154}Dy and ^{156}Er nuclei.

Tab. VIII: Shows the comparison between the calculated energy levels of some negative parity bands in MeV and their corresponding experimental data for ^{154}Dy, ^{156}Er, ^{164}Yb, ^{164}Hf, and ^{166}W [25].

Excitation Energy	^{154}Dy		^{156}Er		^{164}Yb		^{164}Hf		^{166}W	
I^{π}	Exp.	^{12}C	*Exp.*	^{12}C	*Exp.*	^{12}C	*Exp.*	^{12}C	*Exp.*	^{12}C
1^-		0.946		1.067		0.864		0.705		0.858
3^-	1.207	1.223	1.303	1.326		1.118		0.957		1.157
5^-	1.545	1.466	1.611	1.574	1.442	1.373	1.520	1.250	1.587	1.393
7^-	1.964	1.858	2.029	1.967	1.674	1.758	1.836	1.650	1.928	1.792
9^-	2.421	2.267	2.490	2.356	1.999	2.132	2.245	2.170	2.337	2.292
11^-	2.882	2.777	2.924	2.847	2.400	2.618	2.698	2.716	2.742	2.826
13^-	3.390	3.297	3.433	3.372	2.863	3.121	3.155	3.342	3.173	3.454
15^-	3.982	3.912	4.035	3.946	3.377	3.687	3.700	4.026	3.722	4.108
17^-	4.642	4.532	4.711	4.568	3.941	4.299	4.335	4.738	4.378	4.820
19^-	5.338	5.192	5.495	5.202	4.552	4.912	5.009	5.476	5.114	5.557
$\chi^2 - test$		0.036		0.080		0.205		0.422		0.240

One can notice the results of the calculations of the isotopes of any element have good agreement with experimental data when the mass number of parent nucleus increases. One can notice that, a good agreement between the theoretical and experimental energy levels in case of the transitional and rotational nuclei with increasing the neutrons number for the considered transition metal and rare-earth nuclei. It can be shown from the obtained results that ^{12}C as a cluster are better than ^{14}C as a cluster, since ^{12}C is more stable than ^{14}C . Fig.(3) shows the relation between the measured values of $\sqrt{B(E2)}/A_T^{2/3}$ and (Z_1Z_2/Z_T) according to Eq. (10), where the experimental data are taken from Ref. [27]. The solid line is the best fit of the data. The gradient$= r_0^2/\sqrt{4\pi}$, so that $r_0 = 3$ fm and the intercept $a_0 = -8.4361$.

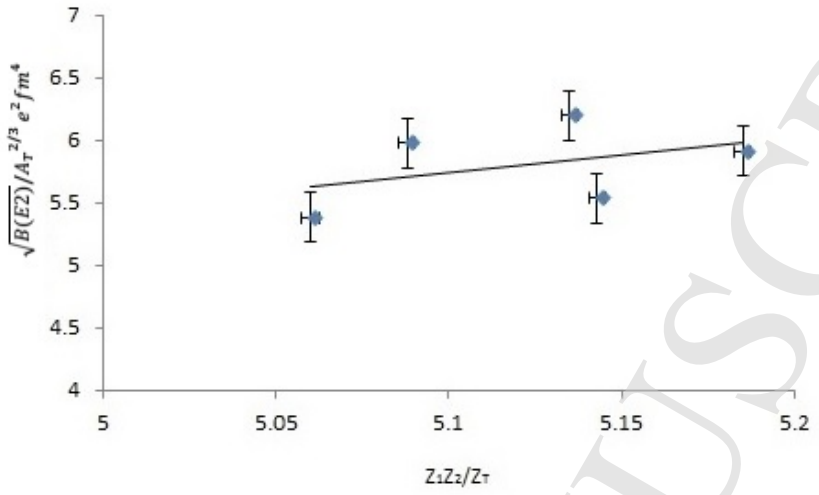

Fig. 3: Shows the plot of the measured values of $\sqrt{B(E2)}/A_T^{2/3}$ versus (Z_1Z_2/Z_T).

IV. CONCLUSION

In the present work, the applicability of using the core-cluster model in the rare-earth and the transition metal regions for even-even nuclei is investigated. The energy levels of the vibrational nuclei (such as ^{154}Dy, ^{156}Er and ^{160}Hf), of the transitional nuclei (such as ^{160}Yb, ^{162}Hf and ^{164}W) and the rotational nuclei (such as ^{160}Dy, ^{162}Er and ^{164}Yb) are studied. The function $D(1,2)$, is used to determine the core-cluster decompositions of the considered nuclei. One notices that, the suitable cluster charge is 6 where, ^{12}C and ^{14}C clusters are considered. One can notice that, the ^{12}C cluster results gives more agreement with the experimental data, according to χ^2-values. The calculations of the core-cluster model are more accurate in describing the ground-state rotational band in case of transitional and rotational nuclei than the vibrational one. Also, the core-cluster model is used to study the spectra of negative parity bands for some selected isotopes where, the values of the first negative energy states are predicted. The core-cluster charges are correlated to the measured $B(E2)$ values to predict the r_0-value. Therefore, the core-cluster model can be used in testing its applicability on vibrational, transitional and rotational regions for heavy deformed nuclei.

[1] B. Buck, A. C. Merchant, and S. M. Perez, Phys. Rev. C 51.559 (1995)
[2] B. Buck, A. C. Merchant, and S. M. Perez, Phys. Rev. C 52, 1840 (1995).
[3] S. Ohkabo, Suppl. Prog. Theor. Phys. 132,1 (1998).
[4] B. Buck, A. C. Merchant, and S. M. Perez, Phys. Rev. Lett. 76,380 (1996).
[5] B. Buck, A. C. Merchant, and S. M. Perez, Nucl. Phys. A 617,195 (1997).
[6] B. Buck, A. C. Merchant, and S. M. Perez, Phys. Rev. C 59, 750(1999).
[7] T. M. Shneidman, G. G. Adamian, N. V. Antonenko, R. V. Jolos, and W. Scheid, Phys. Lett. B 526, 322 (2002).
[8] T. M. Shneidman, G. G. Adamian, N. V. Antonenko, R. V. Jolos, and W. Scheid, Phys. Rev. C 67, 014313 (2003).
[9] G. G. Adamian, N. V. Antonenko, R. V. Jolos, and T. M. Shneidman, Phys. Rev. C 70, 064318 (2004).
[10] T. M. Shneidman, G. G. Adamian, N. V. Antonenko, and R. V. Jolos, Phys. Rev. C 74, 034316 (2006).
[11] T. M. Shneidman, G. G. Adamian, N. V. Antonenko, R. V. Jolos, and Shan-Gui Zhou, , Phys. Rev. C 92, 034302 (2015).
[12] B. Buck, A.C. Merchant, M.J. Horner, and S.M. Perez, Nucl. Phys. A 673, 157(2000).
[13] B. Buck, A.C. Merchant, and S.M. Perez, Phys. Rev. C 57,R 2095 (1998).
[14] B. Buck, A. C. Merchant, S. M. Perez, and H. E. Seals, Phys. Rev. C 76, 014310 (2007).
[15] L.I. Abou-Salem and K. E. Abd El Mageed, Acta Phys. Pol. B 36, No. 6, 2105 (2005).
[16] K. E. Abd El Mageed and A. G. Shalaby, Chin. J. Phys. 53, No. 2, 040301-1 (2015).
[17] B. Buck, A. C. Merchant, M. J. Horner, and S. M. Perez, Phys. Rev. C 61, 024314 (2000).
[18] B. Buck, A. C. Merchant, V. A. McBride, and S. M. Perez,J. Phys. G 30, 1371 (2004).

[19] L. V. Savalyev, "Fundamentals of Theoretical Physics" Vol. 2, Mir Publisher, Moscow (1982).
[20] T. T. Ibrahim, S. M. Perez, S. M. Wyngaadr, B. Buck and A. C. Merchant, Phys. Rev. C 85, 044313 (2012).
[21] B. Buck, A. C. Merchant, and S. M. Perez, J. Phys. G: Nucl. Part. Phys.35,085101(2008).
[22] B. Buck, A. C. Merchant, and S. M. Perez, Phys. Rev. C 85, 054302 (2012).
[23] B. Buck, A. C. Merchant, and S. M. Perez, Phys. Rev. C 77, 017301 (2008).
[24] Dennis Bonatsos, Phys. Rev. C 31, 2256 (1985).
[25] https://www.nndc.bnl.gov/nudat2/reColor.jsp?newColor=e4de2.
[26] G.Audia,A.H.Wapstra, and C.Thibault.Nucl. Phys. A 729,337 (2003).
[27] S.Roman,C.W.Nestor,J.R., and P.Tikkanen atomic data and unclear data tables 78,1-128, (2001).